

Autologous Mesenchymal Stem Cell Therapy for Idiopathic Pulmonary Fibrosis and Comprehensive Assessment of Circulating Immune Populations Cells

Elena Atanasova

Mayo Clinic College of Medicine and Science

Dragana Milosevic

Mayo Clinic College of Medicine and Science

Svetlana Borschlegl

Mayo Clinic College of Medicine and Science

Karen Krucker

Mayo Clinic College of Medicine and Science

Eapen Jacob

Mayo Clinic College of Medicine and Science

Eva Carmona Porquera

Mayo Clinic College of Medicine and Science

Dagny Anderson

Mayo Clinic College of Medicine and Science

Ashley Egan

Mayo Clinic College of Medicine and Science

Andrew Limper

Mayo Clinic College of Medicine and Science

Allan Dietz (✉ dietz.allan@mayo.edu)

Mayo Clinic College of Medicine <https://orcid.org/0000-0003-3410-9621>

Research

Keywords: Autologous adipose mesenchymal stem cells, Characterization, Idiopathic Pulmonary Fibrosis, Treatment, Immunologic profiling

Posted Date: June 9th, 2021

DOI: <https://doi.org/10.21203/rs.3.rs-570630/v1>

Abstract

Background

Idiopathic pulmonary fibrosis (IPF) is a chronic, progressive pulmonary disease characterized by aberrant tissue remodeling, formation of scar tissue within the lungs and continuous loss of lung function. The areas of fibrosis seen in lungs of IPF patients share many features with normal aging lung with cellular senescence being one. The contribution of the immune system to the etiology of IPF remains poorly understood. Evidence obtained from animal models and human studies suggests that innate and adaptive immune processes can orchestrate existing fibrotic responses. Currently, there is only modestly effective pharmacotherapy for IPF. Mesenchymal stem cells (MSCs)-based therapies have emerged as a potential option treatment of IPF. This study explores the possibility of using autologous MSCs as an IPF therapy and present an attempt to determine if the disease occurring in the lungs can be reflected on peripheral blood immune status.

Methods

Comprehensive characterization of autologous adipose derived MSCs (aMSCs) from five IPF patients and five age and gender matched Healthy Controls (HC) was done using flow cytometry, Droplet Digital PCR (ddPCR), Multiplex Luminex xMAP technology and confocal microscopy. For assessing the self renewal capacity and osteogenic differentiation IncuCyte Live Cell Imaging technology was used.

Multi-parameter quantitative flow cytometry of un-manipulated whole blood of another group of 15 IPF patients and 87 (30 age and gender matched) HC was used to analyze 110 peripheral phenotypes.

Results

There are no differences between autologous aMSCs from IPF patients and HC in their stem cell properties, self renewal capacity, plasticity for osteogenic differentiation, secretome content, cell cycle inhibitor marker levels and mitochondrial health.

IPF patients had altered peripheral blood immunophenotype including reduced B cells subsets, increased T cell subsets, and increased granulocytes among others demonstrating clear and significant differences.

Conclusions

Our results indicate that there is no difference in aMSCs properties from IPF patients and HC, suggesting that autologous aMSCs may be an acceptable option for IPF therapy.

Characterization of peripheral immune phenotype may be a valuable indicator for successful therapy, and for potentially staging the disease.

Background

Idiopathic Pulmonary Fibrosis (IPF) is a complex disorder caused by multiple injuries to lung epithelium which triggers a local immune response leading to dysregulation of cellular homeostasis [1]. Accumulations of extracellular matrix and scar formation in IPF are consequences of impaired wound repair mechanisms [2, 3, 4]. The pathogenesis is still poorly understood, and with the exception of lung transplantation, currently there are no significantly effective pharmacotherapies for IPF [2, 5-8]. Growing bodies of evidence from basic science and translational research indicate that IPF appears to be a direct result of immune dysregulation and aberrant wound healing response in the lungs [2, 9, 10]. Not much is known about the contribution of the immune system to the development of IPF or how lung immune responses affect the systemic immunity. To the best of our knowledge, there are no studies which comprehensively investigate the immune status of IPF patients, although there are a few studies identifying potential leukocytes involved with IPF pathogenesis [8, 11-15].

MSCs are important regulators of tissue repair and wound healing processes, have anti-inflammatory properties and display significant immunomodulatory capacity [16]. Use of MSCs-based therapy has emerged as a potential option for treatment of IPF. We have developed an expansive clinical program [17-21] evaluating the therapeutic index of autologous and allogeneic MSCs in a variety of conditions, none of which have evaluated patients with chronic progressive fibrosis. There are promising results of preclinical [22-24] and clinical studies [25-28] using allogeneic MSCs in assessing their safety for IPF treatment. However, the use of autologous adipose MSCs has not been investigated as a possible treatment of IPF.

This study explores the suitability of autologous adipose MSCs as a viable therapy for IPF. Furthermore, it is an attempt to determine if the disease occurring in the lungs can reflect on peripheral blood immune status and thus be used to stage the disease as well as monitoring/predicting changes during MSCs therapy.

Materials And Methods

Procedural Factors

IPF patients (group of 5) were identified from Interstitial Lung Diseases Outpatient Clinic by an expert pulmonologist in IPF and other fibrotic diseases of the lung following the ATS/ERS/JRS/ALAT Statement criteria [29]. All aspects of this study involving samples from IPF patients and age and gender matched healthy volunteers were reviewed and approved by the Mayo Clinic Institutional Review Board. All subjects provided written informed consent to participate.

Patients Characteristics for Adipose Tissue collection and MSC isolation

Variable	Characteristics	IPF (n = 5)	Healthy Contol (n = 5)
Age (years)			
	Mean	77.8	74.8
	Range	73-80	61-80
Gender	Male	3	3
	Female	2	2

Isolation, Propagation and Identification of Adipose MSCs (aMSCs)

Abdominal wall adipose tissue (approximately 1.5 - 2.5 g) was obtained under sterile conditions from IPF patients and age and gender matched healthy donors in an outpatient surgical suite. Tissues were processed with two hours of procurement. Cells were expended *ex vivo* according to the protocol based on Standard Operation Procedures for isolation, extraction and expansion of aMSCs analogs for clinical use [30, 31]. In brief, after micro dissection the fat tissue was digested with collagenase Type I at 0.075% w/v, (Worthington Biochemicals, Lakewood, NJ) for 1.5 h at 37°C. Adipocytes were separated from the vascular fraction by centrifugation (400 x g for 5 min, at room temperature). The cell pellet was washed with PBS and passed through cell strainers (70µm followed by 40µm, BD Biosciences, Franklin Lakes, New Jersey). The resulting cell fraction was plated in T-75 cm² flasks (Thermo Fisher, Waltham, MA) and incubated in a fully humidified incubator supplied with 5%CO₂ in PLGold xeno-free media. The xeno-free media named "PLGold media" consists of: Advanced MEM (Thermo Fisher Scientific) supplemented with 5% (v/v) PLTGold, (Mill Creek Life Sciences, Rochester, MN), 1% (v/v) GlutaMax (Thermo Fisher) and 1% (v/v) antibiotics (100 U/ml penicillin, 100 g/ml streptomycin, HyClone, Logan, UT). Cells were propagated when they were 60-80% confluent using TrypLE (Trypsin-like Enzyme, Invitrogen, Carlsbad, CA) [30]. Cell yield and viability was quantified using Acridine Orange (AO) and *Propidium Iodide* (PI) nuclear stains for exclusion assay on a Luna-FL Dual Fluorescence Cell Counter (all from Logos Biosystems, Annandale, VA). All aMSCs used in the experimental procedures were between passages two and five.

The proliferation and growth rate of aMSCs, was monitored by adding IncuCyte NuCLight Rapid Red Reagent for Nuclear Labeling at 1:500 dilution (Essen Bioscience, Ann Arbor, MI) to the media. After a 30-minute incubation at 37°C in a fully humidified incubator supplied with 5% CO₂, it was placed in the IncuCyte S3 Live Cell Analysis instrument (Sartorius, Ann Arbor, MI) for fluorescent quantification of cell proliferation. Fluorescent images of red nuclei from sixteen fields in each well were captured at 681nm every six hours with 10x objective. Each cell count was repeated twice in four replicas. The data acquisition, visualization and analysis were done using internal IncuCyte S3 Analyzing Software. The growth rate kinetic and doubling times (t_d) were evaluated recording the cell proliferation rate by counting

the number of red nuclei every six hours for a duration of five days. The population doubling time (t_d) was calculated by computing the linear regression of $N=N_0 \times e^{kt}$, where N is the number of red nuclei count at time t, N_0 is red nuclei count at time t = 0, and k is cell growth rate per hour.

Cell phenotype was analyzed by labeling them with primary fluorochrome-conjugated monoclonal antibodies, as previously described [30, 32, 33]. Samples were analyzed using the Beckman Coulter Gallios 3-laser, 10-color flow cytometer and Kaluza 2.1 software (Beckman Coulter, Chaska, MN).

The antibody used, fluorophores, vendors, catalog numbers and dilutions are listed in Table 1.

Table 1: List of antibodies used for identifying aMSCs

Assay	Channel	Antibody	Company	Product ID	Antibody volume (μ) per 1x10 ⁶ cells*
MSC	FITC	CD90	Beckman Coulter	IM1839U	20
	PE	CD73	BD Biosciences	550257	20
	ECD	HLA DR	Beckman Coulter	IM3636	5
	PC5.5	CD14	Beckman Coulter	A70204	5
	PC7	CD105	Beckman Coulter	B43293	10
	APC	HLA-ABC	E-Bioscience	17-9983-42	5
	PBE	CD44	Beckman Coulter	B37789	10
	KRO	CD45	Beckman Coulter	A96416	10
MSC CD3 Controls	FITC	CD3	Beckman Coulter	IM1281U	20
	PE	CD3	BD Biosciences	340662	20
	ECD	CD3	Beckman Coulter	IM2705U	5
	PC5.5	CD3	Beckman Coulter	A66327	5
	PC7	CD3	Beckman Coulter	6607100	10
	APC	CD3	Beckman Coulter	IM2467U	10
	PBE	CD3	Beckman Coulter	A93687	10
	KRO	CD3	Beckman Coulter	B00068	10

* The antibodies are added into the samples without dilution, as per manufacturer instructions.

Morphologic Characterization

Cells were seeded at 6100 cells/cm² in a sterile eight well chamber (Cellvis, Sunnyvale, CA) for 48 hours. Fresh media containing 350 nM MitoTracker Red CXMRos (Invitrogen) was added to the cells and incubated 30 minutes in a fully humidified incubator supplied with 5% CO₂, followed by washing with PBS. Cells were fixed by adding 10% buffered Formalin (Azer Scientific, Morgantown, PA). The covered glass chambers wrapped in aluminum foil were kept for 30 minutes on a rocker at room temperature. PBS washed cells were permeabilized with 0.3% TRITON X-100 in PBS containing Hoechst 33342 (1:1000 dilution, Thermo Fisher) and AlexaFluor™ 488 Phalloidin (1:1500 dilution, Thermo Fisher). Aluminum foil wrapped covered glass chambers were kept for 30 minutes on a rocker at room temperature. Cells were washed with PBS and kept in PBS to prevent them from drying during imaging.

A laser scanning confocal microscope was used to collect 2D and 3D cell images LSM 780 and ZEN 2010 software (Carl Zeiss, NY). For quantification of the cells mitochondrial volume five individual aMSCs from each cell line [total 25 cells from Healthy Controls (HCaMSCs) and 25 cells from IPF patients (IPFaMSCs)] were imaged under the same acquisition conditions: image size (512 x 512 pixels), number of Z-stack slices (16 slices, 7.692 mm), number of averaging Z-stack slices (averaging 2 Z-stack slices), scan zoom (X: 1.0, Y: 1.0), pinhole sizes and laser intensities (1.42 AU for 405 nm laser at 50% intensity, 1.19 AU for 488 nm laser at 50% intensity, and 0.99 AU for 561 nm laser at 40% intensity) using C-Apochromat 63x/1.2W Korr objective.

Detection was carried out at wavelengths of 406-480 nm for Hoechst 33342 (nuclear stain), 499-560 nm for AlexaFluor™ 488 Phalloidin (actin F stain) and 566-696 nm for MitoTracker Red CXMRos (mitochondria stain). For image analysis and mitochondria volume calculations Image Data Management Software Imaris 8 (Oxford Instruments, Abingdon, GB) was used. Unpaired Student t-test analysis was used to determine the statistical difference in mitochondria volumes between aMSCs of the two tested groups.

Adipogenic Differentiation Capacity

Cells, passages 2 and 3, previously cultured in PLGold media, were cultured for two consecutive passages in MSC NutriStem® XF Basal Medium containing MSC NutriStem® XF Supplement Mix (named “MSC NutriStem® XF Medium” Biological Industries, Cromwell, CT) supplemented with 5% (v/v) PLTGold before seeding at 5260 cells/cm² in a CellBIND 24 well plate (Corning, Corning NY). After 4 days, media in the wells with cells assigned for adipogenesis was replaced with MSCgo™ Adipogenic Differentiation Medium (Biological Industries, Cromwell, CT) containing Adipogenic Differentiation Supplement Mix I and Adipogenic Differentiation Supplement Mix II (Biological Industries). Control cultures were maintained in MSC NutriStem® XF Medium. Cells were kept for six days in the respected media, changing media once before adding fresh respected media containing 1:500 dilution of IncuCyte NucLight Rapid Red Reagent for Nuclear Labeling and 1:1000 dilution of LipidSpot™ 488 Lipid Droplet Stain (Biotium, Fremont, CA). After 30 min incubation at 37⁰C in a fully humidified incubator supplied with 5% CO₂ plates were placed in an IncuCyte S3 Live Cell Analysis instrument for red nuclei count and green lipid droplets total green integrated intensity (GCU) imaging using 20 x objective. Fluorescent images of red nuclei (imaged at 681 nm) and green lipid GCU (imaged at 585 nm) from 16 fields in each well were captured every six hours for 24 hours. The data acquisition, visualization and analysis were done using internal IncuCyte S3 Analyzing Software. Each GCU value per well was normalized to the number of cells (red nuclei count) per well.

Secretome Analysis of Resting aMSCs

aMSCs were seeded at 2105 cell/cm² in 6 well plates with 2.5 ml PLGold media/well. After 48 hours, the media was replaced with 2 ml fresh media/well. One well containing media only was used as a control for media content of analytes, which values were used as a background in secretome analysis.

After four days (96 h), media was collected, spun for five minutes at 750 x g and supernatants were stored at -20°C until use. Immediately after collecting the media, 1 ml of fresh media containing 1:500 diluted IncuCyte NucLight Rapid Red Reagent was added to the cells. Cell number (red nuclei count) was counted in an IncuCyte S3 Live Cell Analysis instrument. For determining aMSCs secretome content, a 20plex custom made kit (Human Cytokine/Chemokine, Human Bone and Adipokine Magnetic bead panel, EMD Millipore, Burlington, MA), and Luminex xMAP technology (R&D Systems Inc., Minneapolis, MN) were used. The secretome assay was done in triplicate and was performed following the manufacturer's instructions. The plates were read by the MAGPIX instrument using xPONENT software for acquisition (Luminex, Austin, TX). Data analysis of the Median Fluorescence Intensity (MFI) and Coefficient of Variance (CV%) estimation were done by MILLIPLEX Analyst 5.1 software (EMD Millipore). The analyte concentrations (pg/ml) were normalized to 1x10⁶ cells.

Analysis of aMSCs Senescence Status by Droplet Digital Polymerase Chain Reaction (ddPCR)

For establishing the senescence status of aMSCs we developed a Droplet Digital PCR (ddPCR) protocol for estimating the transcription level of CDKN1, p16^{INK4A}, p53, and RB1 cell cycle inhibitor markers. Total RNA from 1.5 x 10⁶ cell pellets was extracted using RNeasy Mini Kit (Qiagen, Germantown, MD). The reverse transcription reaction was performed with random, Oligo(dT)₂₀, primers using iScript cDNA Synthesis Kit (Bio-Rad, Hercules, CA). For ddPCR reactions fluorescent labeled custom designed primers and probe for p16^{INK4A}:

p16^{INK4A} forward primer: 5' GCC CAA CGC ACC GAA TAG 3',

p16^{INK4A} reverse primer: 5' ACG GGT CGG GTG AGA GTG 3', and

p16^{INK4A} probe: FAM6-TCA TGA TGA TGG GCA GCG CC-TAMRAIowaBlack, (IDT, Coralville, IA) were used.

For the other tested cell cycle inhibitor markers as well as for TATA Binding Protein (TBP) as reference gene, commercially available fluorescent labeled expression primers and probes were used (Bio-Rad).

The ddPCR reaction setup was as previously described [34]. The final concentration of primers and probes in the reactions were 900 nmol/L and 250 nmol/L, respectively. Multiwall plates were sealed, vortexed briefly, centrifuged and placed on an automated droplet generator (AutoDG- Bio-Rad). Each sample was partitioned into 15,000-20,000 droplets. PCR amplification was performed on a Veriti Thermal Cycler (Applied Biosystems). The initial heating at 95°C for 10 minutes was followed by 60

cycles of denaturation at 94°C for 30 seconds, annealing and extension at 58°C for 1 minute, and a final extension step at 98°C for 10 minutes. The completed reactions were stored at 4°C until reading them on a QX200 droplet reader (Bio-Rad). Data analysis was performed using 2D Module of the QuantaSoft software (BioRad).

Quantitative Flow Cytometry Assay for Immunoprofiling

Procedural Factors

A separate group of 15 IPF patients were identified from the Interstitial Lung Diseases Outpatient Clinic by an expert pulmonologist in IPF and other fibrotic diseases of the lung following the ATS/ERS/JRS/ALAT Statement criteria [29]. All aspects of this study involving samples from IPF patients and age and gender matched healthy volunteers were reviewed and approved by the Mayo Clinic Institutional Review Board. All subjects provided written informed consent to participate.

Table 2. Demographic characteristics and lung function indices

Variable	Characteristics	IPF patients (n =15)	Healthy Control	Healthy Control
			Age 50+ (n =30)	All (n=87)
Age (years)	Mean ± STD	76 ± 6.94	56 ± 3.74	40 ± 13.32
	Range	65-89	50-69	19-69
Gender	Female	6	7	20
	Male	9	23	67
Lung Function				
FVC% predictive		73 ± 15.6		
FEV1% predictive		85.2±14.1		
VC _{max} % predictive		74.2±15.1		
Treatment at immunophenotyping (n)				
Pirfenidone		5		
Nintedanib		2		
Prednisone		1		
No medications		7		

Data are presented as mean ± SD, FVC% predictive = % of Forced Vital Capacity; FEV1% predictive = % of Forced Expiratory Volume in the 1st second, predictive; VC_{max} % predictive = % Maximal Vital capacity.

“Predictive” means values adjusted for patient age, gender, and race.

To characterize the circulating immune phenotype, peripheral blood samples from 87 healthy volunteers (30 of which age and gender matched) and from a separate group of 15 IPF patients were collected in K₂EDTA tubes (Becton Dickinson, Franklin Lakes, NJ) at initial or return visits. Un-manipulated whole blood was stained with antibodies directly within 12 hours of collection. Appropriate antibodies, undiluted (vendors, catalog numbers and amounts added per sample are listed in Additional File 1 and in [35, 36])

were added directly to the blood samples. Quantitative flow cytometry was performed to comprehensively assess 110 leukocyte populations and phenotypes from lymphocytes, monocytes, and granulocytes. All 10-color procedures, antibodies, flow protocols, instrument settings, and gating strategies for peripheral blood flow cytometry have been previously described by Gustafson et al. [35, 36]. The flow cytometry data were analyzed using Kaluza 2.1 software (Beckman Coulter), allowing quantification of the absolute number as well as percent of immune cell subtypes. Fluorescently labeled isotypes were used as a control for each tested cell line.

Statistical Analysis

Results are expressed as mean \pm SD. Statistical analysis was performed using GraphPad Prism 8 software. Intergroup comparisons of parametrically distributed continuous data were done using unpaired two-tailed Student's *t*-test. Differences were considered significant when *p* values **p*<0.05, ***p*<0.01, ****p*<0.001, *****p*<0.0001. Correlations between IPF patients' Pulmonary Function Test (PFT) values were established by calculating the Pearson correlation coefficient (*r*). Flow cytometry data are either represented as percentage of population or number of cells/ml. ddPCR data and presented as mean of three with CV%.

Discussion

In this study we explore the possibility of using autologous adipose MSCs as an IPF therapy. MSC's mode of action is still not fully understood, but they target the sites of injury, inhibit inflammation, and contribute to epithelial tissue repair [17–21, 24, 41]. Promising results of preclinical studies using MSCs suggest that they may represent a potential therapeutic option for the treatment of chronic lung diseases including IPF [22–24]. Few clinical trials have been reported using adult allogeneic MSCs of different sources for treatment of IPF. Tzouveleakis et al. conducted a non-randomized, no placebo-controlled, phase 1b clinical trial to assess the safety of the allogeneic adipose MSCs in treatment of IPF [25]. Chambers et al. reports using placental MSCs in a clinical 1b study on a small cohort of IPF patients [26]. Glassberg et al. was using bone marrow derived MSCs in a phase I safety clinical trial [27]. Averyanov et al. reports that in phase I/IIA clinical study high cumulative doses of bone marrow MSCs were used [28]. All of the clinical trials so far demonstrate that use of MSCs in IPF treatment are safe and well tolerated, even in the case when an extremely high dose of MSCs was used [28]. Although MSCs are immune privileged and MSCs therapies are well tolerated without serious adverse events there have been reported few minor side effects (fever and chills), which were contributed to the allogeneic nature of MSCs.

Subcutaneous adipose tissues MSCs are frequently used for clinical applications because of their easy access, minimally invasive procedure and their therapeutic potentials having been extensively studied [30, 42].

This study examines the biological phenotype of adipose aMSCs isolated from IPF patients (IPFaMSCs) and age and gender matched healthy controls (HCaMSCs) expanded in PLGold xeno-free media to

establish their suitability for IPF treatment.

Comprehensive characterization of aMSCs from both groups was carried out using a combination of flow cytometry, ddPCR, confocal microscopy, IncuCyte Live Cell Imaging and LUMINEX xMAP technologies. Our data provides evidence that autologous adipose tissue derived MSCs from IPF patients exhibit the same properties as the adipose tissue derived MSCs from the HC. (i) the aMSCs were adherent to plastic and exhibited the same small, spindle shape morphology, (ii) all tested cell lines were more than 99% positive for typical MSCs markers, and negative for lineage markers expression [32, 37, 38], (iii) the growth curves of IPFaMSCs and HCaMSCs cell lines display three distinct phases: initial short lag phase, followed by exponential growth and finally the plateau phase which is in agreement with the general behavior of the MSCs [43]. All cell lines have comparable exponential growth and have the same doubling times, which indicates identical potency for self-renewal, (iv) all aMSCs display similar health status, evaluated by analyzing the cells and mitochondrial morphology and assessing mitochondrial volumes. Changes in mitochondrial volume have been associated with a wide range of important biological functions and pathologies [44]. Current evidence suggests that the areas of fibrosis seen in IPF patients' lungs share many mitochondrial dysfunction features [45]. The mitochondria of both tested cell lines have a typical shape and distribution for healthy MSCs mitochondria [46]. The IPFaMSCs mitochondrial volume is not different from the mitochondrial volume of HCaMSCs, which indicates that IPFaMSCs are healthy, not in a state of stress and are fully functional, (v) the capacity and plasticity for adipogenic differentiation of IPFaMSCs was the same as of HCaMSCs, (vi) MSCs are known to interact and actively communicate with their surrounding microenvironment through the secretion of cytokines and growth factors. Both cell groups secrete the same amount of growth factors, anti-inflammatory as well as pro-inflammatory cytokines, which indicates that the cell lines from both groups have the same capacity for regulating the tissue regeneration, proliferation, angiogenesis and modulation of inflammation, (vii) it has been long recognized that cellular senescence significantly contributes to the aging-related declines in tissue regeneration capacity and in the pathogenesis of aging-related diseases, such as IPF. The mechanism of how senescent cells contribute to aging and aging-related diseases remains unclear. Resident stem cells are particularly sensitive to senescence stresses. One of the hypotheses is that cellular senescence leads to exhaustion of the resident stem cells, which, in turn, causes a decline in tissue regenerative capacity during aging or upon injury [47].

The findings in our study are that IPFaMSCs have the same expression profile of cell cycle marker inhibitors as HCaMSCs and that there are no present senescence features in IPFaMSCs caused by the disease.

While establishing the suitability of using autologous aMSCs for IPF treatment, we also wanted to find out whether an organ disease, as it is in the case of lungs with IPF, is reflected on the systemic immunity. To do so, we assessed the immune status of IPF patients by quantifying their circulating phenotypes and compared them with healthy controls. In addition, we sought to identify changes in IPF patients' immunological phenotypes, which correlate with their lung function indices.

Circulating granulocytes, neutrophils and eosinophils were found elevated in IPF patients' blood. These cells are first to respond to the presence of pathogens in human lungs or upon tissue damage. They migrate from periphery to the damaged lungs in response to secreted chemokine and interleukin signals from invaded lungs and become activated [48, 49]. They were found elevated in bronchoalveolar lavage fluid (BALF) and sputum of IPF patients [50], as well as in peripheral blood, sputum and BALF in chronic obstructive pulmonary disease (COPD) patients [11]. Granulocytes and neutrophil counts in IPF patients in our study inversely correlate with all three measured pulmonary indices. High levels of neutrophil elastase were found in lung parenchyma and in both BALF and IPF patient serum. Therefore, neutrophils might indeed play an important role in the pathogenesis of IPF [51]. The same result was found in IPF patients BALF along with the increased IL-8 concentrations [50], and it was speculated that those findings might be predictive for future exacerbations of IPF [52]. There is evidence that neutrophils might promote fibrosis *via* their regulation of extra cellular matrix (ECM) turnover [51, 53, 54]. Kinder et al. reports that an increased number of neutrophils in BALF is associated with early mortality in IPF [55]. All of these effects/interactions are complex and multifaceted and are not fully studied or understood in the case of IPF.

Natural Killer (NK) cells are the most important cell subsets involved in the production of IFN- γ , a cytokine suggested to improve survival of IPF patients [56, 57]. In our study, only the percentage of [CD56 + CD16-] NK cells in IPF patients' blood is elevated in comparison with HCs. A high percentage of this subset of NK cells was also observed in the blood of bone marrow transplant patients [58]. The functional study of isolated [CD56 + CD16-] cells indicates that these cells have very low cellular toxicity [58]. The dynamic nature of cytokine and cellular profile of the microenvironment influences the development of specific NK subtypes which may lead to conversion from pro-inflammatory to pro-resolution NK subtypes [59]. If there is any defect or disturbance in this process, it may lead to more severe inflammation and eventually to airway damage which can be reflected in the circulating phenotypes [12].

Recent studies have shown that B cells, as part of adaptive immunity, are involved in IPF pathology [13, 60]. In our study there is no difference in the total number of B cells and the percentage of Plasma B cells between two tested groups. However, the Transitional B cells were lower in IPF patients than in HCs. As immature B cells emigrate from the bone marrow and enter the blood stream, they migrate toward the wounded organ (the lungs in the case of IPF) being attracted by secreted chemokines from the wounded lungs [13]. This can explain our findings of decreased circulating Transitional B cell percentage in IPF patients' blood. At the same time our measurements of circulating [CD27 + IgM-IgD-] cell percentage shows an increase in IPF patients. It has been found that stimulated [CD27 + IgM-IgD-] cells activate telomerase and are responsible for age-related exhaustion of the B cells [14, 61, 62]. Since immune exhaustion and telomerase dysfunction have been implicated in IPF pathology, this subset of B-cells may be a good topic for further research.

In contrast to [CD27 + IgM-IgD-] cells, the number as well as the percentage of [CD27 + IgM + IgD+] cells in the IPF patients' blood were reduced. The reduced amount of this B cell subpopulation has been found in

the blood of sarcoidosis patients [63] and in patients with common variable immunodeficiency (CVID) with recurrent lower respiratory tract infections [64]. Studying the functional capacity of these cells in early inflammatory responses Seifert et al. concluded that [CD27 + IgM + IgD+] memory B cells are generated in T cell-dependent immune response [65]. The exact role of this B cell subpopulation in IPF pathology is not elucidated yet.

The role of T cells in the pathology of pulmonary fibrosis is poorly understood and controversial. It was hypothesized that if IPF progression depends on an adaptive immune component, it would be possible to find associations between phenotypic changes of circulating T cells and clinical manifestations of the disease [58]. Current evidence suggests that there are substantial T cell subset abnormalities in the blood [66–68], peripheral blood proteome profile [68], BALF [69, 70] and lung tissue in IPF patients [71, 72] which may contribute to the fibrotic processes. In our study, the total number of circulating T cells in IPF patients does not differ from HCs, but there is a difference in T helper cells as well as in cytotoxic / suppressor T cell subpopulations. Five [CD4+] subpopulation T helper cells have increased percentages in comparison to HCs of which [CD4 + CD25 + Tregs] are most studied. Patients with IPF had larger fractions of these circulating cells and they are inversely correlated with all three measured pulmonary indices. Our results are in agreement with findings of Hou et al. [66]. An increase in circulating [CD4 + CD25 + Tregs] cells is a hallmark of disturbed immune homeostasis in various pulmonary diseases, including IPF [73]. A lower proportion of regulatory [CD25 + CDRA + Treg] cells in IPF patients in our study are in agreement with the findings in other studies where a low proportion of these cells have been detected in blood and BALF of IPF patients [66, 74]. A low percentage of regulatory T cells have limited inhibitory activity, and hence impaired immune tolerance [74].

The involvement of T helper and cytotoxic/suppressor cell subsets in the pathology of IPF has been poorly understood (74). The increased percentage of [CD4 + CTLA4+], [CD4 + CTLA4 + CD28+], [CD8 + PD-1+], [CD8 + CTLA4+] and [CD8 + CTLA4 + CD28+] indicate that there is substantial down regulation in immune response in IPF patients [75].

Monocytes are known to contribute to the pathogenesis of idiopathic pulmonary fibrosis as was shown in the retrospective, multicenter cohort study [76]. The robust association of high monocyte count associated with mortality in other fibrotic diseases suggests they might contribute to the pathogenesis of these diseases as well. In our study, IPF patients have a higher percentage of circulating [CD33+] monocytes, which may contribute to the progression of the disease.

Conclusion

MSCs-based therapies for IPF, so far, are using allogeneic cells for treatment. Although the safety and tolerance of their use was confirmed, there are still minor side effects present, which might be circumvented by using autologous MSCs. Our study shows that adipose MSCs from IPF patients are not part of IPF pathology and may be used for IPF therapy.

Understanding the immunological status of IPF patients may provide insight into their immunity and its role in etiology of the disease. To our knowledge, our study is the most comprehensive evaluation of circulating phenotype in IPF patients so far and provides further evidence for the role of adaptive immunity in the pathogenesis of IPF. The increased Tregs in the IPF patients' peripheral blood correlate inversely with disease severity. Treg subpopulations may be promising prognostic factors for IPF. Characterization of the peripheral immune phenotypes in IPF patients may answer the question whether or not the immune events identified in the circulation can be used: as a monitor for personalized IPF therapy, to potentially classify/stage the disease, and identify those more likely to respond to therapy. Additional studies are needed with an expanded cohort of patients for positive identification of circulating phenotypes from peripheral blood as potential biomarkers for IPF.

Abbreviations

aMSCs: Adipose tissue derived mesenchymal stem cells; AO: Acridine Orange; ATS/ERS/JRS/ALAT: American Thoracic Society/ European Respiratory Society/ Japanese Respiratory Society/ Latin American Thoracic Society; CDKN1/p21CIP1: Cyclin-dependent kinase inhibitor 1; COPD: Chronic obstructive pulmonary disease; CV%: Coefficient of variance %; CVID: Common variable immune deficiency; ddPCR: Droplet digital polymerase chain reaction; ECM: Extracellular matrix; FEV1: Forced expiratory volume during first second; FVC: *Forced vital capacity*; GCU: Total green integrated intensity; HCs: Healthy controls; HCaMSCs: Healthy controls adipose mesenchymal stem cells; IPF: Idiopathic pulmonary fibrosis; IPFaMSCs: Idiopathic pulmonary fibrosis patients adipose mesenchymal stem cells; MFI: Mean fluorescent intensity; MEM: Modified Eagle medium; MSCs: Mesenchymal stem cells; p16^{ink4a}: cyclin-dependent kinase inhibitor 2A; NK: Natural killer cells; p53: Cellular tumor antigen p53; PBS: Phosphate-buffered saline; PFT: Pulmonary function test; PI: *Propidium iodide*; PLGold: Human platelet lysate; PCR: Polymerase chain reaction; K₂EDTA: Di-potassium ethylenediaminetetraacetic acid; RB1: Retinoblastoma transcriptional corepressor 1; RNA: Ribonucleic Acid; SD: Standard deviation; TBP: TATA binding protein; VC_{max}: Maximal vital capacity

Declarations

Ethics Approval and Consent to Participate

Mayo Clinic IRB has reviewed and approved both the protocol and consent form used to enroll patients and healthy volunteers into this protocol to obtain the appropriate biological samples.

Consent for Publication

Not applicable

Availability of Data and Materials

All data are fully available without restriction.

All relevant data are within the manuscript and its Additional data files.

Competing Interests

I have read the Journal's policy and the authors for this manuscript have the following competing interests: ABD is the inventor of technology used as a tool in this research.

The technology is not the focus of this work, but may benefit from positive results of this work. The technology has been licensed to Mill Creek Life Sciences, and Mayo Clinic and ABD have contractual rights to receive royalties from the licensing of this technology. In addition, Mayo Clinic and ABD hold equity in the company to which the technology is licensed. This conflict is managed according to policies and procedures regarding conflict of interest at Mayo Clinic.

This does not alter our adherence to Stem Cell Research & Therapy policies on sharing data and materials.

Funding

We graciously acknowledge the generous gift to ABD from the Thomas Hurvis Foundation specifically given for research in the use of autologous mesenchymal cells as a therapy for Idiopathic Pulmonary Fibrosis, which made this study possible, and for funds from the 2019 Research Award which was awarded to ABD by the Department of Laboratory Medicine and Pathology at Mayo Clinic, Rochester, MN. The funders did not play any role in the study design, data collection and analysis, decision to publish, or preparation of the manuscript.

Authors' Contributions

Conceptualization and designed the experiments: EA and ABD

Identifying IPF patients for the samples collection: AHL and EMC

Consenting IPF patients for participation and fat tissue extraction: KPK

Healthy Volunteers identification and consenting for participation: EKJ

Pulmonary functional tests performing: DKA and AME

Droplet Digital PCR design, experiments, and analysis: DM

Quantitative Flow cytometry immunoprofiling assay and analysis: SB

Design, performed experiments and data analysis: EA

Wrote the manuscript: EA, ABD

Acknowledgements

Not applicable

References

1. Fernandez IE, Eickelberg O. New cellular and molecular mechanisms of lung injury and fibrosis in idiopathic pulmonary fibrosis. *The Lancet*. 2012;380(9842):680–8.
2. Betensley A, Sharif R, Karamichos D. A systematic review of the role of dysfunctional wound healing in the pathogenesis and treatment of idiopathic pulmonary fibrosis. *Journal of clinical medicine*. 2017;6(1):2.
3. Ryu JH, Moua T, Daniels CE, Hartman TE, Eunhee SY, Utz JP et al, editors. Idiopathic pulmonary fibrosis: evolving concepts. Mayo Clinic Proceedings; 2014. Elsevier.
4. Foronjy RF, Majka SM. The potential for resident lung mesenchymal stem cells to promote functional tissue regeneration: understanding microenvironmental cues. *Cells*. 2012;1(4):874–85.
5. King TE Jr, Albera C, Bradford WZ, Costabel U, Hormel P, Lancaster L et al. Effect of interferon gamma-1b on survival in patients with idiopathic pulmonary fibrosis (INSPIRE): a multicentre, randomised, placebo-controlled trial. *The Lancet*. 2009;374(9685):222–8.
6. Raghu G, Brown KK, Costabel U, Cottin V, Du Bois RM, Lasky JA et al. Treatment of idiopathic pulmonary fibrosis with etanercept: an exploratory placebo-controlled trial. *American journal of respiratory and critical care medicine*. 2008;178(9):948–55.
7. Network IPFCR. Prednisone, azathioprine, and N-acetylcysteine for pulmonary fibrosis. *N Engl J Med*. 2012;366(21):1968–77.
8. Feghali-Bostwick CA, Tsai CG, Valentine VG, Kantrow S, Stoner MW, Pilewski JM, et al. Cellular and humoral autoreactivity in idiopathic pulmonary fibrosis. *The Journal of Immunology*. 2007;179(4):2592–9.
9. Desai O, Winkler J, Minasyan M, Herzog EL. The role of immune and inflammatory cells in idiopathic pulmonary fibrosis. *Frontiers in medicine*. 2018;5:43.

10. Shenderov K, Collins SL, Powell JD, Horton MR. Immune dysregulation as a driver of idiopathic pulmonary fibrosis. *Journal of Clinical Investigation*. 2021.;131(2):e143226.
11. Freeman CM, Crudgington S, Stolberg VR, Brown JP, Sonstein J, Alexis NE. et.al. Design of a multi-center immunophenotyping analysis of peripheral blood, sputum and bronchoalveolar lavage fluid in the Subpopulations and Intermediate.
12. Outcome, Measures. in COPD Study (SPIROMICS). *Journal of translational medicine*. 2015;13(1):19.
13. Esposito I, Perna F, Ponticiello A, Perrella M, Gilli M, Sanduzzi A. Natural killer cells in BAL and peripheral blood of patients with idiopathic pulmonary fibrosis (IPF). *International journal of immunopathology and pharmacology*. 2005.;18(3):541–5.
14. Xue J, Kass DJ, Bon J, Vuga L, Tan J, Csizmadia E, et al. Plasma B lymphocyte stimulator and B cell differentiation in idiopathic pulmonary fibrosis patients. *The Journal of Immunology*. 2013;191(5):2089–95.
15. Heukels P, van Hulst JA, van Nimwegen M, Boersma CE, Melgert BN, Jan H. et.al. Enhanced Bruton's tyrosine kinase in B-cells and autoreactive IgA in patients with idiopathic pulmonary fibrosis. *Respiratory research*. 2019;20(1):232.
16. Asai Y, Chiba H, Nishikiori H, Kamekura R, Yabe H, Kondo S, et al. Aberrant populations of circulating T follicular helper cells and regulatory B cells underlying idiopathic pulmonary fibrosis. *Respiratory research*. 2019;20(1):1–9.
17. Uccelli A, Moretta L, Pistoia V. Mesenchymal stem cells in health and disease. *Nature reviews immunology*. 2008;8(9):726–36. Singer W, Dietz AB, Zeller AD, Gehrking TL, Schmelzer. Schmeichel JD AM, et.al. Intrathecal administration of autologous mesenchymal stem cells in multiple system atrophy. *Neurology*. 2019;93(1):e77–87.
18. Dietz AB, Dozois EJ, Fletcher JG, Butler GW, Radel D, Lightner AL et al. Autologous mesenchymal stem cells, applied in a bioabsorbable matrix, for treatment of perianal fistulas in patients with Crohn's disease. *Gastroenterology*. 2017.;153(1):59–62. e2.
19. Saad A, Dietz AB, Herrmann SM, Hickson LJ, Glockner JF, McKusick MA, et al. Autologous mesenchymal stem cells increase cortical perfusion in renovascular disease. *J Am Soc Nephrol*. 2017;28(9):2777–85.
20. Dozois EJ, Lightner AL, Mathis KL, Chua HK, Kelley SR, Fletcher JG, et al. Early results of a phase I trial using an adipose-derived mesenchymal stem cell-coated fistula plug for the treatment of transsphincteric cryptoglandular fistulas. *Diseases of the Colon. & Rectum*. 2019;62(5):615–22.
21. Bydon M, Dietz AB, Goncalves S, Moinuddin F, Alvi MA, Goyal A et al, editors. CELLTOP clinical trial: first report from a phase 1 trial of autologous adipose tissue-derived mesenchymal stem cells in the treatment of paralysis due to traumatic spinal cord injury. *Mayo Clinic Proceedings*; 2020: Elsevier.
22. Ortiz LA, Gambelli F, McBride C, Gaupp D, Baddoo M, Kaminski N et al. Mesenchymal stem cell engraftment in lung is enhanced in response to bleomycin exposure and ameliorates its fibrotic effects. *Proceedings of the*.
23. National Academy of Sciences. 2003;100(14):8407–11.

24. Limper AH. Safety of IV human mesenchymal stem cells in patients with idiopathic pulmonary fibrosis. *Chest*. 2017;151(5):951–2.
25. Tzouvelekis A, Toonkel R, Karampitsakos T, Medapalli K, Ninou I, Aidinis V. et.al. Mesenchymal stem cells for the treatment of idiopathic pulmonary fibrosis. *Frontiers. Medicine*. 2018;5:142.
26. Tzouvelekis A, Paspaliaris V, Koliakos G, Ntoliou P, Bouros E, Oikonomou A, et.al. A prospective, non-randomized, no placebo-controlled, phase Ib clinical trial to study the safety of the adipose derived stromal cells-stromal vascular fraction in idiopathic pulmonary fibrosis. *Journal of translational medicine*. 2013;11(1):171.
27. Chambers DC, Enever D, Ilic N, Sparks L, Whitelaw K, Ayres J, et al. A phase 1b study of placenta-derived mesenchymal stromal cells in patients with idiopathic pulmonary fibrosis. *Respirology*. 2014;19(7):1013–8.
28. Glassberg MK, Minkiewicz J, Toonkel RL, Simonet ES, Rubio. DiFede GA D, et.al. Allogeneic human mesenchymal stem cells in patients with idiopathic pulmonary fibrosis via intravenous delivery (AETHER). a phase I safety clinical trial. *Chest*. 2017;151(5):971–81.
29. Averyanov A, Koroleva I, Konoplyannikov M, Revkova V, Lesnyak V, Kalsin V. et.al. First-in-human high-cumulative-dose stem cell therapy in idiopathic pulmonary fibrosis with rapid lung function decline. *Stem cells translational medicine*. 2020;9(1):6–16.
30. Raghu G, Collard HR, Egan JJ, Martinez FJ, Behr J, Brown KK, et al. An official ATS/ERS/JRS/ALAT statement: idiopathic pulmonary fibrosis: evidence-based guidelines for diagnosis and management. *American journal of respiratory and critical care medicine*. 2011;183(6):788–824.
31. Dudakovic A, Camilleri E, Riester SM, Lewallen EA, Kvasha S, Chen X, et al. High-resolution molecular validation of self-renewal and spontaneous differentiation in clinical-grade adipose-tissue derived human mesenchymal stem cells. *Journal of cellular biochemistry*. 2014;115(10):1816–28.
32. Crespo-Diaz R, Behfar A, Butler GW, Padley DJ, Sarr MG, Bartunek J et al. Platelet lysate consisting of a natural repair proteome supports human mesenchymal stem cell proliferation and chromosomal stability. *Cell transplantation*. 2011;20(6):797–812.
33. Dominici M, Le Blanc K, Mueller I, Slaper-Cortenbach I, Marini F, Krause D et al. Minimal criteria for defining multipotent mesenchymal stromal cells. The International Society for Cellular Therapy position statement. *Cytotherapy*. 2006;8(4):315–7.
34. Camilleri ET, Gustafson MP, Dudakovic A, Riester SM, Garces CG, Paradise CR. et al. Identification and validation of multiple cell surface markers of clinical-grade adipose-derived mesenchymal stromal cells as novel release criteria for good manufacturing practice-compliant production. *Stem cell research & therapy*. 2016;7(1):107.
35. Milosevic D, Mills JR, Campion MB, Vidal-Folch N, Voss JS, Halling KC et al. Applying standard clinical chemistry assay validation to droplet digital PCR quantitative liquid biopsy testing. *Clinical chemistry*. 2018;64(12):1732–42.
36. Gustafson MP, Lin Y, Maas ML, Van Keulen VP, Johnston PB, Peikert T, et al. A method for identification and analysis of non-overlapping myeloid immunophenotypes in humans. *PloS one*.

2015;10(3).

37. Gustafson MP, DiCostanzo AC, Wheatley CM, Kim C-H, Bornschlegl S, Gastineau DA, et al. A systems biology approach to investigating the influence of exercise and fitness on the composition of leukocytes in peripheral blood. *Journal for immunotherapy. of cancer.* 2017;5(1):30.
38. Gustafson MP, Staff NP, Bornschlegl S, Butler GW, Maas ML, Kazamel M et al. Comprehensive immune profiling reveals substantial immune system alterations in a subset of patients with amyotrophic lateral sclerosis. *PloS one.* 2017;12(7).
39. Gustafson MP, Lin Y, LaPlant B, Liwski CJ, Maas ML, League SC, et al. Immune monitoring using the predictive power of immune profiles. *Journal for immunotherapy of cancer.* 2013;1(1):7.
40. Taylor SC, Laperriere G, Germain H. Droplet Digital PCR versus qPCR for gene expression analysis with low abundant targets: from variable nonsense to publication quality data. *Scientific reports.* 2017;7(1):1–8.
41. Van Heetvelde M, Van Looke W, Trypsteen W, Baert A, Vanderheyden K, Crombez B, et al. Evaluation of relative quantification of alternatively spliced transcripts using droplet digital PCR. *Biomolecular detection and quantification.* 2017;13:40 – 8.
42. Mundra V, Gerling IC, Mahato RI. Mesenchymal stem cell-based therapy. *Molecular pharmaceuticals.* 2013;10(1):77–89.
43. Chu D-T, Nguyen Thi Phuong T, Tien NLB, Tran DK, Minh. Thanh LB VV, et al. Adipose tissue stem cells for therapy. An update on the progress of isolation, culture, storage, and clinical application. *Journal of clinical medicine.* 2019;8(7):917.
44. Colter DC, Sekiya I, Prockop DJ. Identification of a subpopulation of rapidly self-renewing and multipotential adult stem cells in colonies of human marrow stromal cells. *Proceedings of the National Academy of Sciences.* 2001;98(14):7841–5.
45. Kaasik A, Safiulina D, Zharkovsky A, Veksler V. Regulation of mitochondrial matrix volume. *American Journal of Physiology-Cell Physiology.* 2007;292(1):C157-C63.
46. Wanet A, Arnould T, Najimi M, Renard P. Connecting mitochondria, metabolism and stem cell fate. *Stem Cells Dev.* 2015;24(17):1957–71. Seo BJ, Yoon SH, Do JT. Mitochondrial dynamics in stem cells and differentiation. *Int J Mol Sci.* 2018;19(12):3893.
47. Liu R-M, Liu G. Cell senescence and fibrotic lung diseases. *Experimental Gerontology.* 2020;132:110836.
48. Futosi K, Fodor S, Mócsai A. Reprint of Neutrophil cell surface receptors and their intracellular signal transduction pathways. *International immunopharmacology.* 2013;17(4):1185–97.
49. Mayadas TN, Cullere X, Lowell CA. The multifaceted functions of neutrophils. *Annual Review of Pathology. Mechanisms of Disease.* 2014;9:181–218.
50. Ashitani J-i, Mukae H, Taniguchi H, Ihi T, Kadota J-i, Kohno S et al. Granulocyte-colony stimulating factor levels in bronchoalveolar lavage fluid from patients with idiopathic pulmonary fibrosis. *Thorax.* 1999;54(11):1015–20.

51. Obayashi Y, Yamadori I, Fujita J, Yoshinouchi T, Ueda N, Takahara J. The role of neutrophils in the pathogenesis of idiopathic pulmonary fibrosis. *Chest*. 1997;112(5):1338–43.
52. Car BD, Meloni F, Luisetti M, Semenzato G, Gialdroni-Grassi G, Walz A. Elevated IL-8 and MCP-1 in the bronchoalveolar lavage fluid of patients with idiopathic pulmonary fibrosis and pulmonary sarcoidosis. *American journal of respiratory and critical care medicine*. 1994;149(3):655–9.
53. Gregory AD, Kliment CR, Metz HE, Kim KH, Kargl J, Agostini BA et al. Neutrophil elastase promotes myofibroblast differentiation in lung fibrosis. *Journal of leukocyte biology*. 2015;98(2):143–52.
54. Kolahian S, Fernandez IE, Eickelberg O, Hartl D. Immune mechanisms in pulmonary fibrosis. *American journal of respiratory cell and molecular biology*. 2016;55(3):309–22.
55. Kinder BW, Brown KK, Schwarz MI, Ix JH, Kervitsky A, King TE Jr. Baseline BAL neutrophilia predicts early mortality in idiopathic pulmonary fibrosis. *Chest*. 2008;133(1):226–32.
56. Mehrotra PT, Donnelly RP, Wong S, Kanegane H, Geremew A, Mostowski HS et al. Production of IL-10 by human natural killer cells stimulated with IL-2 and/or IL-12. *J Immunol*. 1998;160(6):2637–44.
57. Raghu G, Brown KK, Bradford WZ, Starko K, Noble PW, Schwartz DA, et al. A placebo-controlled trial of interferon gamma-1b in patients with idiopathic pulmonary fibrosis. *N Engl J Med*. 2004;350(2):125–33.
58. Jacobs R, Stoll M, Stratmann G, Leo R, Link H, Schmidt RE. CD16-CD56⁺ natural killer cells after bone marrow transplantation. *Blood*. 1992;79(12):3239–3244.
59. Wehner R, Dietze K, Bachmann M, Schmitz M. The bidirectional crosstalk between human dendritic cells and natural killer cells. *Journal of innate immunity*. 2011;3(3):258 – 63.
60. Todd NW, Scheraga RG, Galvin JR, Iacono AT, Britt EJ, Luzina IG, et al. Lymphocyte aggregates persist and accumulate in the lungs of patients with idiopathic pulmonary fibrosis. *Journal of inflammation research*. 2013;6:63.
61. Colonna-Romano G, Bulati M, Aquino A, Pellicanò M, Vitello S, Lio D, et al. A double-negative (IgD – CD27 –) B cell population is increased in the peripheral blood of elderly people. *Mechanisms of ageing and development*. 2009;130(10):681 – 90.
62. Martorana A, Balistreri CR, Bulati M, Buffa S, Azzarello DM, Camarda C, et al. Double negative (CD19 + IgG + IgD – CD27 –) B lymphocytes: a new insight from telomerase in healthy elderly, in centenarian offspring and in Alzheimer's disease patients. *Immunology letters*. 2014;162(1):303–9.
63. Heaps A, Varney V, Bhaskaran S, Ford B, Mosley A. Patients with Chronic Sarcoidosis have Reduced CD27 + IgM + IgD + Unswitched Memory B cells and an Expanded Population of Terminal Effector CD8 + CD27-CD28-T cells. *J Clin Cell Immunol*. 2012;3(132):2.
64. Carsetti R, Rosado MM, Donnanno S, Guazzi V, Soresina A, Meini A, et al. The loss of IgM memory B cells correlates with clinical disease in common variable immunodeficiency. *Journal of Allergy and Clinical Immunology*. 2005; 115. (2):412–7.
65. Seifert M, Przekopowicz M, Taudien S, Lollies A, Ronge V, Drees B, et al. Functional capacities of human IgM memory B cells in early inflammatory responses and secondary germinal center reactions. *Proceedings of the National Academy of Sciences*. 2015;112(6):E546–E55.

66. Hou Z, Ye Q, Qiu M, Hao Y, Han J, Zeng H. Increased activated regulatory T cells proportion correlate with the severity of idiopathic pulmonary fibrosis. *Respiratory research*. 2017;18(1):170.
67. Gilani SR, Vuga LJ, Lindell KO, Gibson KF, Xue J, Kaminski N, et al. CD28 down-regulation on circulating CD4 T-cells is associated with poor prognoses of patients with idiopathic pulmonary fibrosis. *PloS one*. 2010;5(1).
68. O'Dwyer DN, Norman KC, Xia M, Huang Y, Gurczynski SJ, Ashley SL, et al. The peripheral blood proteome signature of idiopathic pulmonary fibrosis is distinct from normal and is associated with novel immunological processes. *Scientific reports*. 2017;7:46560.
69. Galati D, De Martino M, Trotta A, Rea G, Bruzzese D, Cicchitto G, et al. Peripheral depletion of NK cells and imbalance of the Treg/Th17 axis in idiopathic pulmonary fibrosis patients. *Cytokine*. 2014;66(2):119 – 26.
70. Papiris SA, Kollintza A, Karatza M, Manali ED, Sotiropoulou C, Milic-Emili J, et al. CD 8 + T lymphocytes in bronchoalveolar lavage in idiopathic pulmonary fibrosis. *Journal of Inflammation*. 2007;4(1):14.
71. Nuovo GJ, Hagood JS, Magro CM, Chin N, Kapil R, Davis L, et al. The distribution of immunomodulatory cells in the lungs of patients with idiopathic pulmonary fibrosis. *Modern Pathology*. 2012;25(3):416 – 33.
72. Adegunsoye A, Hrusch CL, Bonham CA, Jaffery MR, Blaine KM, Sullivan M, et al. Skewed lung CCR4 to CCR6 CD4 + T cell ratio in idiopathic pulmonary fibrosis is associated with pulmonary function. *Frontiers in immunology*. 2016;7:516.
73. Singh R, Alape D, de Lima A, Ascanio J, Majid A, Gangadharan SP. Regulatory T Cells in Respiratory Health and Diseases. *Pulmonary Medicine*. 2019;2019.
74. Kotsianidis I, Nakou E, Bouchliou I, Tzouvelekis A, Spanoudakis E, Steiropoulos P, et al. Global impairment of CD4 + CD25 + FOXP3 + regulatory T cells in idiopathic pulmonary fibrosis. *American journal of respiratory and critical care medicine*. 2009;179(12):1121-30.
75. Habel DM, Espindola MS, Kitson C, Azzara AV, Coelho AL, Stripp B, et al. Characterization of CD28 null T cells in idiopathic pulmonary fibrosis. *Mucosal immunology*. 2019;12(1):212 – 22.
76. Scott MK, Quinn K, Li Q, Carroll R, Warsinske H, Vallania F, et al. Increased monocyte count as a cellular biomarker for poor outcomes in fibrotic diseases: a retrospective, multicentre cohort study. *The Lancet Respiratory Medicine*. 2019.;7(6):497–508.

Figures

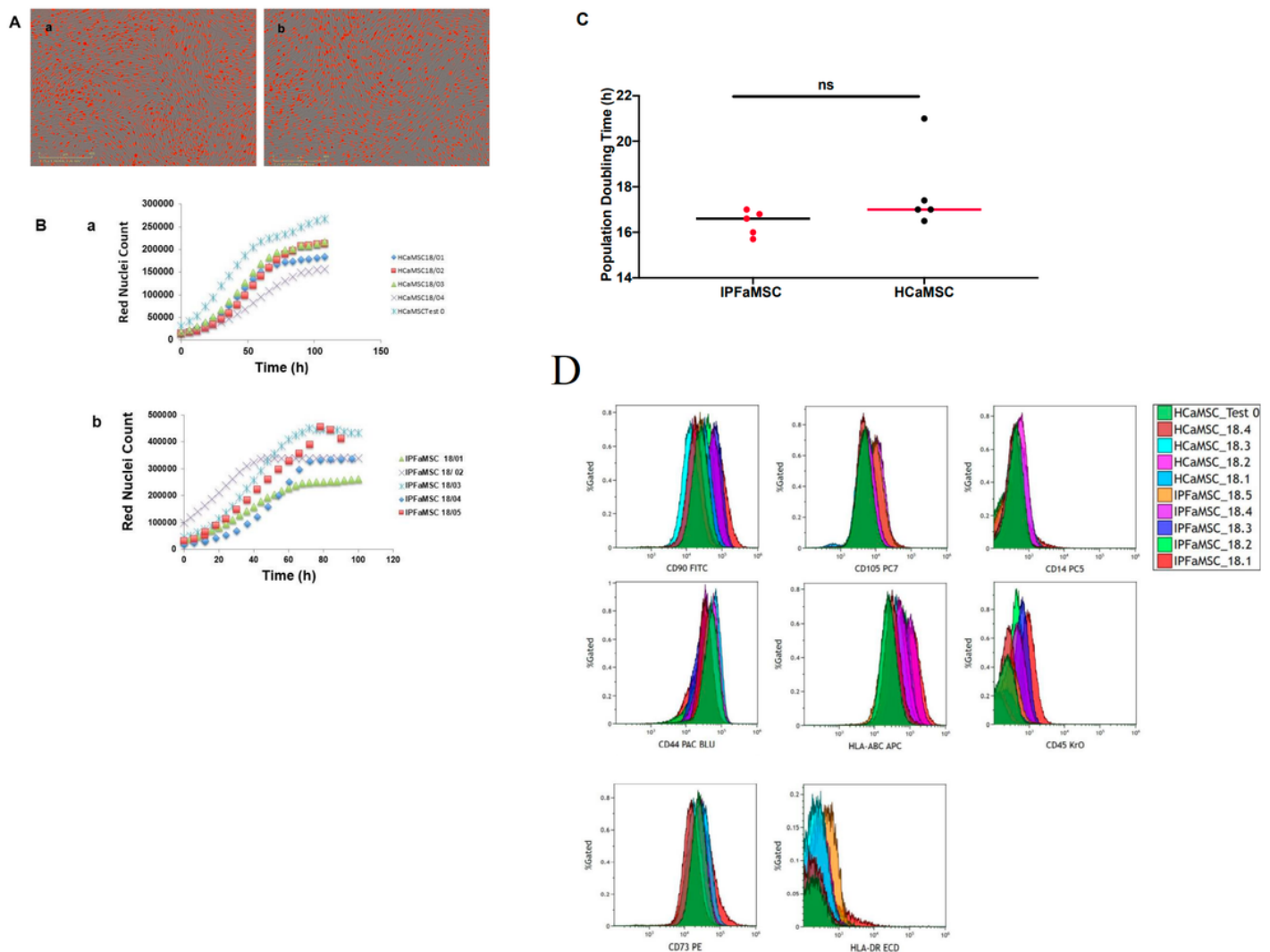


Figure 1

Proliferation, growth rate kinetic, doubling time comparison. A. Representative images of HCaMSCs. (a). and IPFaMSCs. (b). growth for 2 days in IncuCyte S3 Live Cell Analysis instrument. All tested cells lines exhibit spindle-shaped adherent morphology. Nuclei are stained red. B. Cell proliferation rate estimated by counting the number of red nuclei for 5 days. (a). HCaMSCs growth rate kinetics; (b). IPFaMSCs growth rate kinetics C. Unpaired Student t-test analysis of population doubling times of both tested groups. Dots represent individual cell line values. Differences were considered significant when $*p < 0.05$, compared with control cell lines values. D. Flow cytometry results of IPFaMSCs HCaMSCs phenotypes. All ten cell lines tested more than 95% positive for typical MSCs markers CD90, CD73, CD105, CD44 and HLA-ABC expression, and negative for lineage markers CD14, CD45 and HLA-DR expression.

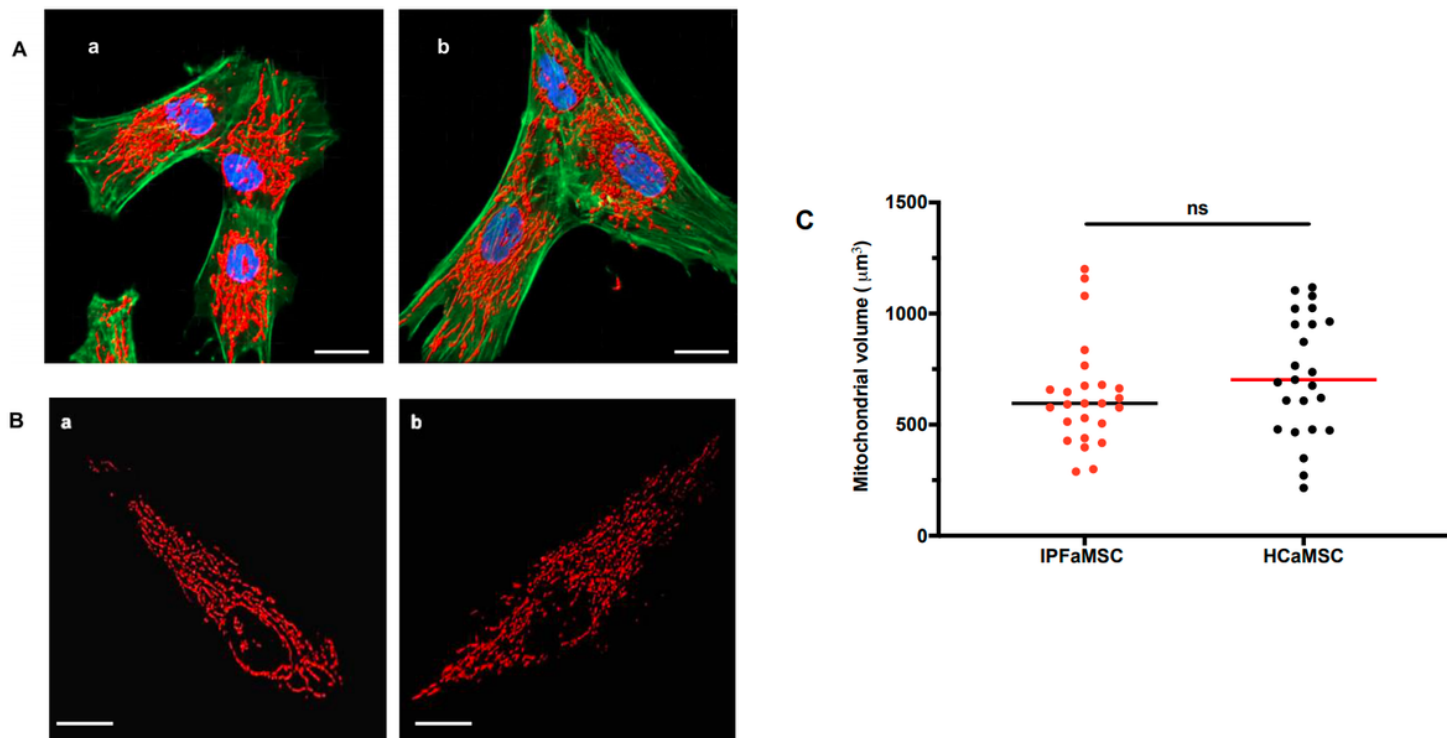


Figure 2

Cell morphology and mitochondrial volume evaluation by laser scanning confocal microscopy. A. Representative fluorescence images of HCaMSCs (a). and (b). IPFaMSCs Scale bar = 20 μm B. Representative images of mitochondria 3D isosurface in HCaMSCs (a) and IPFaMSCs (b) created by Imaris 8 software. Scale bar = 20 μm C. Statistical analysis of mitochondrial volumes was done by unpaired Student t- test. Dots represent individual cell values. Differences were considered significant when $*p < 0.05$, compared with control cell values.

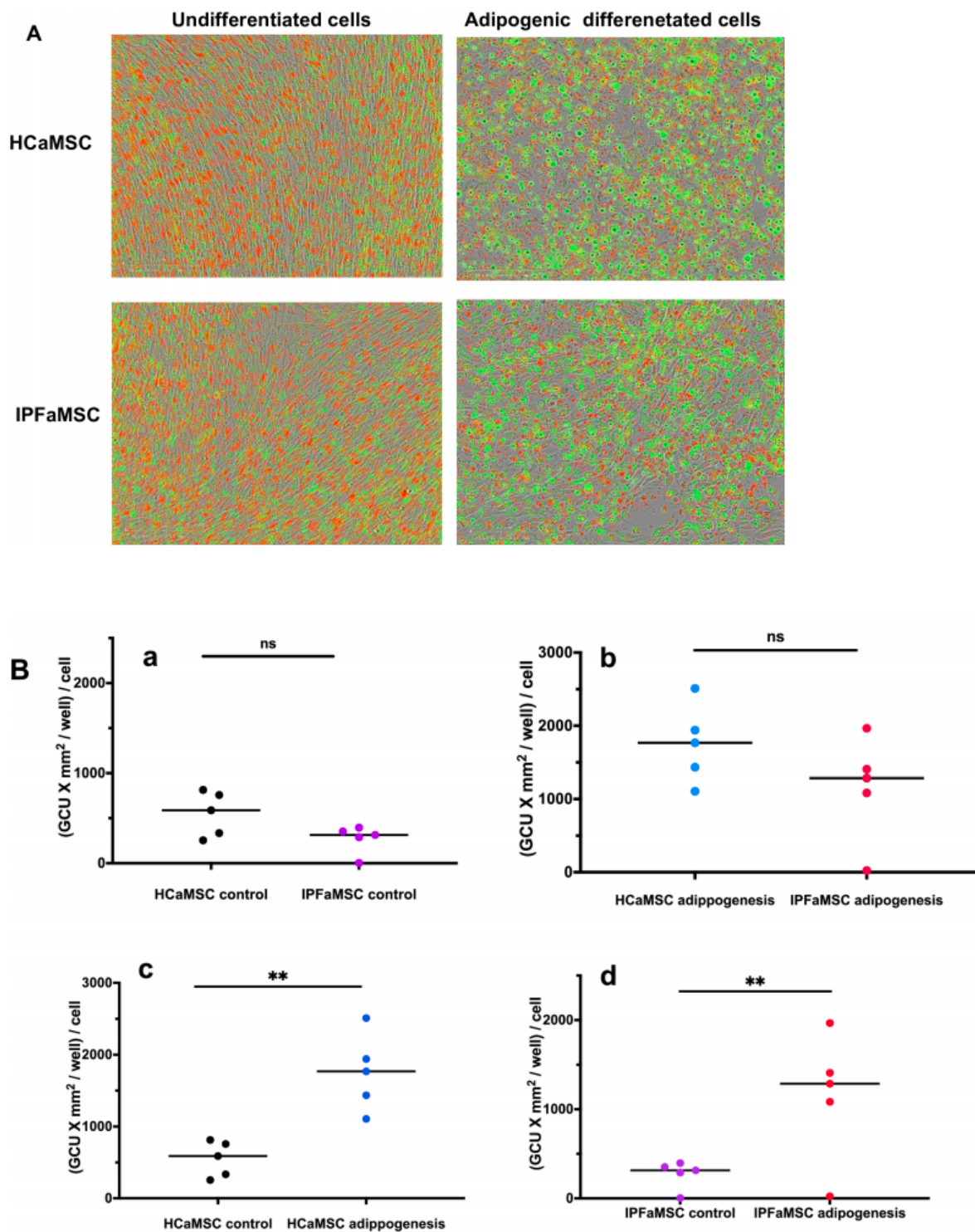


Figure 3

Adipogenic differentiation of IPFaMSCs and HCaMSCs A. Representative images of undifferentiated and adipogenic differentiated (a) HCaMSCs and (b) IPFaMSCs. B. Unpaired Student t-test was used for analyzing the statistical differences of adipogenesis in (a) undifferentiated HCaMSCs and IPFaMSCs. No significant difference in growth rate in non adipogenic media between these two groups was found, with median values of 588 (GCU x mm²/well)/cell and 314 (GCU x mm²/well)/cell respectively. (b) No

significant difference was found between adipogenic capacity of HCaMSCs and IPFaMSCs with median values of 1768 (GCU x mm2/well)/cell and 1287 (GCU x mm2/well)/cell respectively. (c) Significant difference was found between undifferentiated and adipogenic differentiated HCaMSCs as well as (d) between undifferentiated and adipogenic differentiated IPFaMSCs. Dots represent individual cell lines values. ** p<0.01, compared with control cell lines.

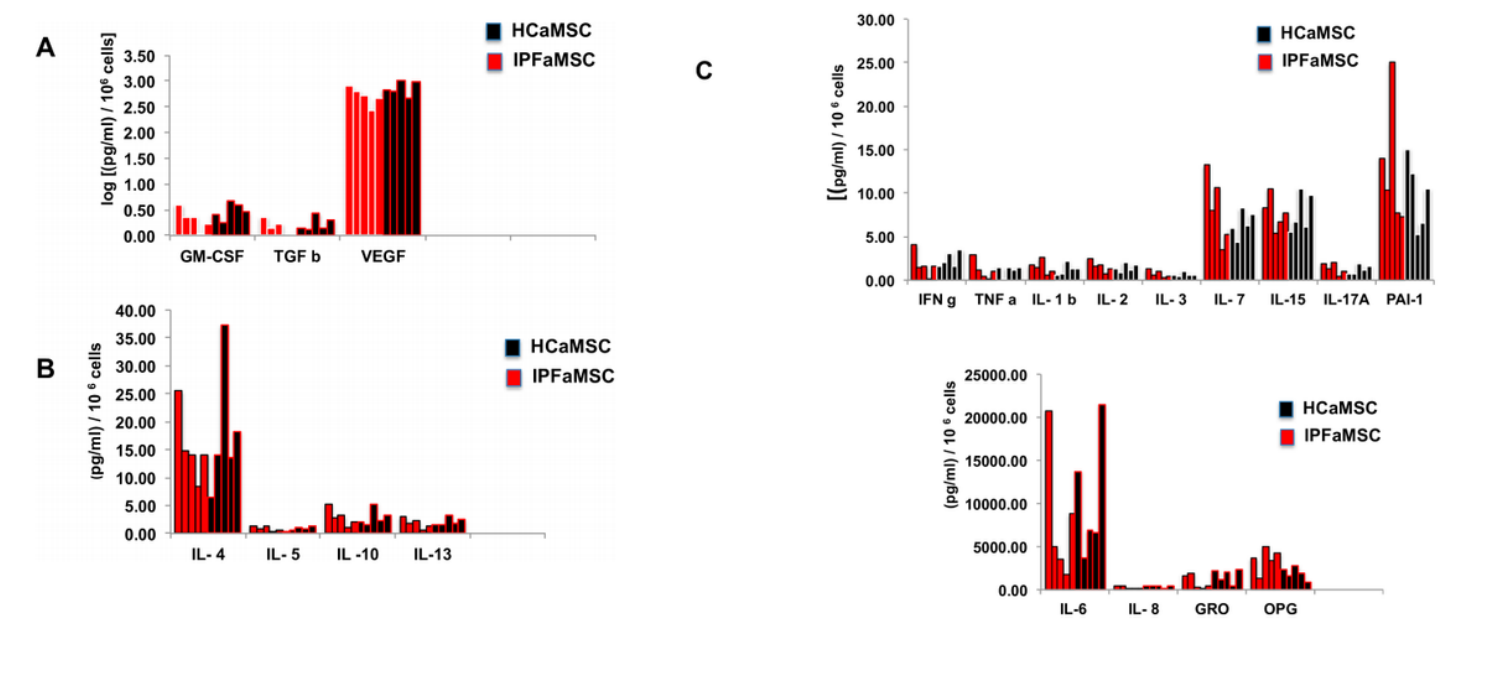


Figure 4

Secretome profile of IPFaMSCs and HCaMSCs. The Luminex assay was performed in triplicate on media collected 4 days after initial incubation of the cells. A. Log value of the secreted growth factors. B. Secreted anti-inflammatory cytokines. C. Secreted pro inflammatory cytokines. CV% was less than 13% for all analytes. The concentrations of analytes (pg/ml) were normalized to the number of cells in each well and expressed as (pg/ml)/1 x10 6 cells.

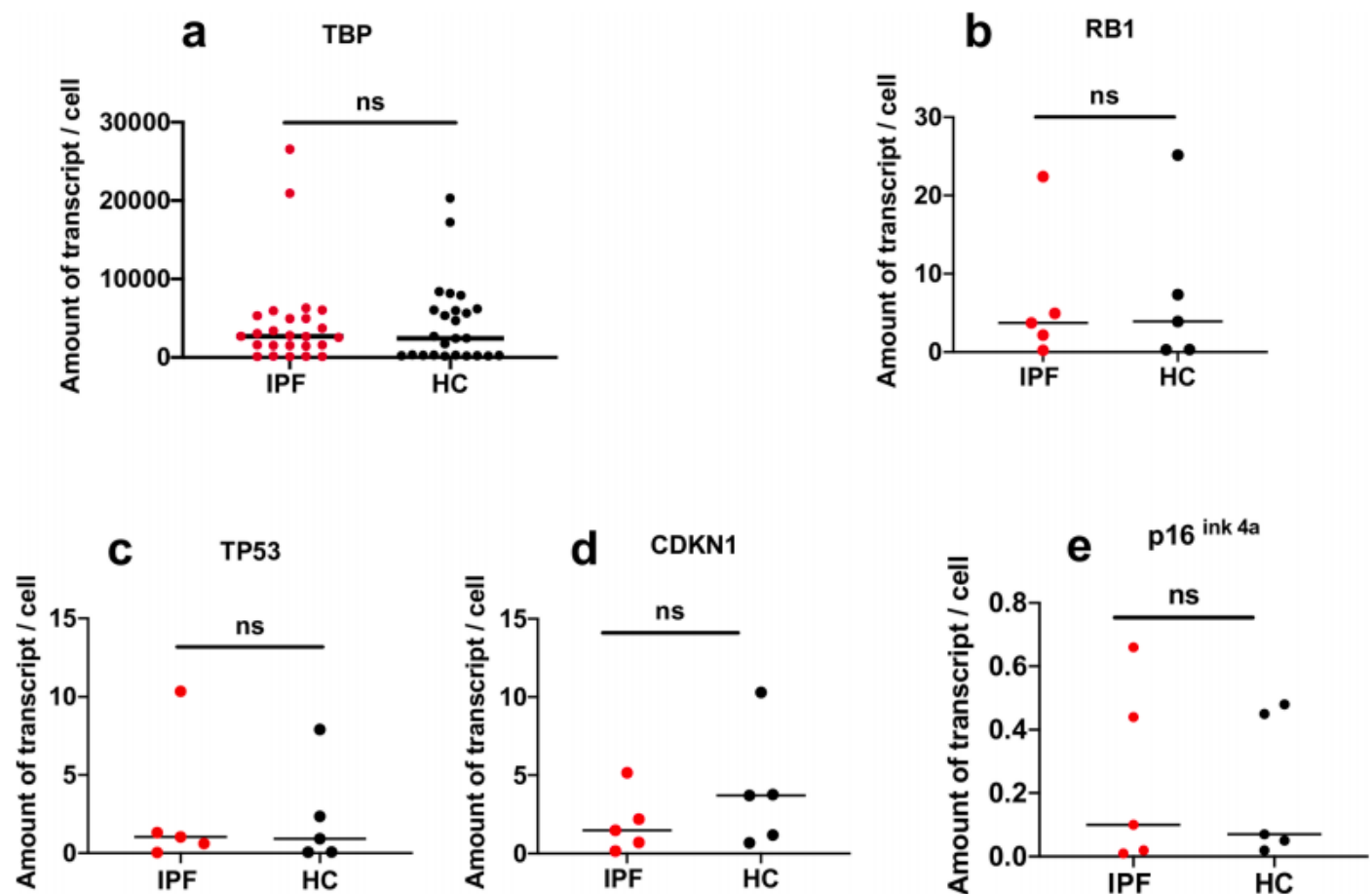


Figure 5

Senescence status of aMSCs. Unpaired Student t- test of cell cycle inhibitor marker transcription levels. The mean values of the tested aMSCs groups for (a) TBP expression for IPFaMSCs and HCaMSCs were 4401 and 4296 transcript amount/cell, respectively. (b) RB1 expression mean values for IPFaMSCs and HCaMSCs were 6.69 and 7.40 transcript amount/cell, respectively. (c) TP53 expression mean values for IPFaMSCs and HCaMSCs were 2.67 and 2.66 transcript amount/cell, respectively. (d) CDKN1 expression mean values for IPFaMSCs and HCaMSCs were 1.96 and 3.93 transcript amount/cell, respectively. (e) p16^{ink4a} expression mean values for IPFaMSCs and HCaMSCs were 0.244 and 0.214 transcript amount/cell, respectively. The CV% between triplicates were less than 15% for all tested transcripts. No significant difference was found in the expression levels of tested cell cycle inhibitor markers. Dots represent individual cell line values. Differences were considered significant when $*p < 0.05$, compared with control cell lines.

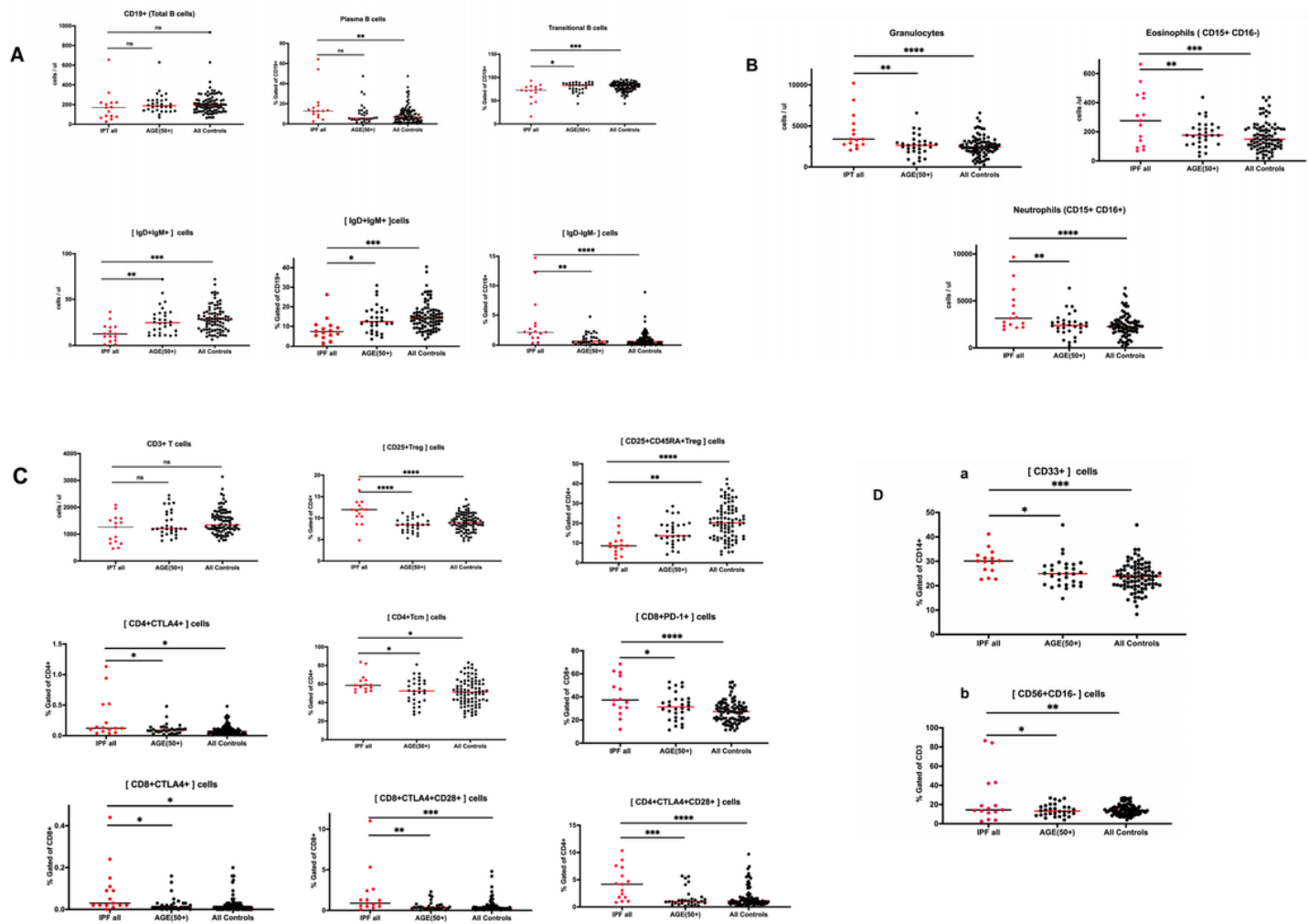


Figure 6

Immunoprofile comparison of blood samples from IPF patients and HCs using unpaired Student t-test. A. B cells panel. There is no difference in total B cell numbers between the tested groups. IPF patients have decreased percentage as well as cell number of [IgD+IgM+] cells, smaller percentage of Transitional B cells, while higher percentage of [IgD-IgM-] cells. B. Granulocytes, Eosinophils and Neutrophils panel. IPF patients have elevated numbers of granulocytes, eosinophils, and neutrophils than HCs. C. T cells panel: Total number of T (CD3+) cells is not different between two groups, while the percentages of [CD4+CTLA4+], [CD4+CTLA4+CD28+], [CD8+CTLA4+], [CD8+CTLA4+CD28+], [CD8+PD-1+] cells as well as [CD25+Treg] and [CD4+Tcm] T cells are elevated. Only the percentage of CD25+CD45RA+Treg cells is decreased. D. Monocytes (a) and Natural Killer cells (b) panel: Both cell phenotypes exhibit higher percentages in IPF patients. Dots represent individual values. *p<0.05, ** p<0.01, *** p<0.001, **** p<0.0001, compared with control group.

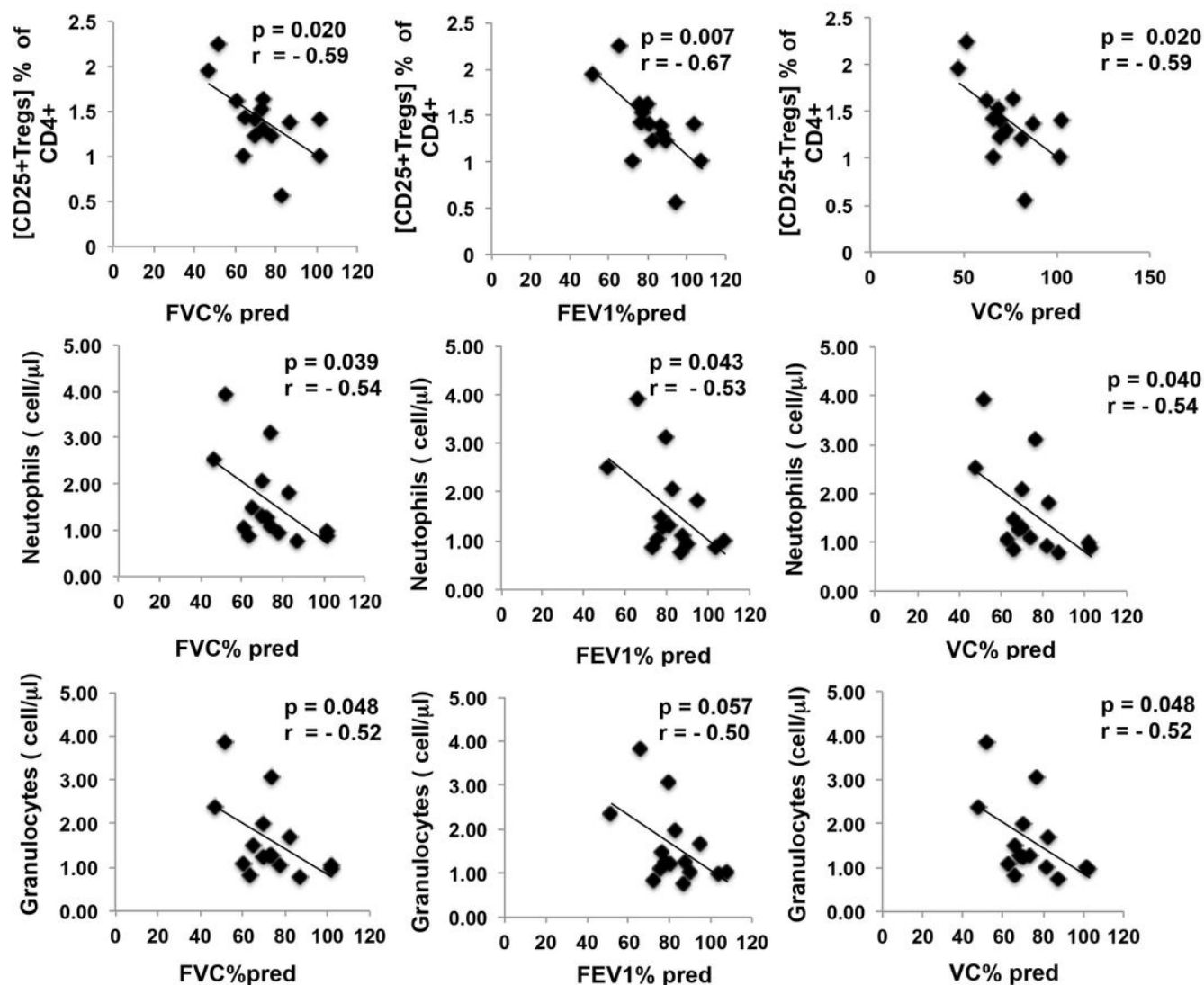


Figure 7

Pearson's correlation coefficients (r) for IPF Phenotype = f (Pulmonary Function Test). Dots represent individual values. Correlation graphs show Pearson correlation coefficient r-value and p-value. p-values were determined by Student's t-test distribution for Pearson correlation. Lines represent the best fit resulting from linear regression analysis. The results are significant at *p < .05

Supplementary Files

This is a list of supplementary files associated with this preprint. Click to download.

- [Additionalfile1.pdf](#)
- [Additionalfile2.pdf](#)
- [Additionalfile3A.pdf](#)
- [AdditionalFile3B.pdf](#)

- [Additionalfile3Ca.pdf](#)
- [Additionalfile3Cb.pdf](#)
- [AdditionalFile4.pdf](#)